

PI3K–mTORC2 but not PI3K–mTORC1 Regulates Transcription of HIF2A/EPAS1 and Vascularization in Neuroblastoma

Sofie Mohlin¹, Arash Hamidian¹, Kristoffer von Stedingk¹, Esther Bridges², Caroline Wigerup¹, Daniel Bexell¹, and Sven Pahlman¹

Abstract

Hypoxia-inducible factor (HIF) is a master regulator of cellular responses to oxygen deprivation with a critical role in mediating the angiogenic switch in solid tumors. Differential expression of the HIF subunits HIF1 α and HIF2 α occurs in many human tumor types, suggesting selective implications to biologic context. For example, high expression of HIF2 α that occurs in neuroblastoma is associated with stem cell–like features, disseminated disease, and poor clinical outcomes, suggesting pivotal significance for HIF2 control in neuroblastoma biology. In this study, we provide novel insights into how HIF2 α expression is transcriptionally controlled by hypoxia and how this control is abrogated by inhibition of insulin-like growth factor-1R/INSR-driven phos-

phoinositide 3-kinase (PI3K) signaling. Reducing PI3K activity was sufficient to decrease HIF2 α mRNA and protein expression in a manner with smaller and less vascularized tumors *in vivo*. PI3K-regulated HIF2A mRNA expression was independent of Akt or mTORC1 signaling but relied upon mTORC2 signaling. HIF2A mRNA was induced by hypoxia in neuroblastoma cells isolated from metastatic patient–derived tumor xenografts, where HIF2A levels could be reduced by treatment with PI3K and mTORC2 inhibitors. Our results suggest that targeting PI3K and mTORC2 in aggressive neuroblastomas with an immature phenotype may improve therapeutic efficacy. *Cancer Res*; 75(21); 1–12. ©2015 AACR.

Introduction

Mammalian cells adapt to hypoxia by activating a transcriptional program orchestrated by the heterodimeric hypoxia-inducible factors (HIF) 1 and 2 via stabilization of their oxygen-sensitive HIF α subunits (1, 2). Tumor hypoxia and HIF1 α and HIF2 α protein expression are associated with aggressive disease, metastasis, resistance to therapy, and thus poor clinical outcome for patients with various cancers (3–9). HIF1 α and HIF2 α share high sequence homology, but it is becoming increasingly evident that HIF1 α and HIF2 α have differential spatial and temporal regulation in response to hypoxia in human tumors and developing tissues (4, 5, 7, 8, 10–12).

Neuroblastoma is a childhood tumor of the developing sympathetic nervous system (SNS). We have previously demonstrated that HIF2 α is expressed in hypoxic areas and within the perivascular niche, where it promotes a local pseudo-hypoxic tumor

phenotype (4, 13). In addition, HIF2 α is a marker of immature, neural crest-like neuroblastoma cells in tumor specimens (13), and high HIF2 α protein expression is associated with aggressive disease and poor clinical outcome in neuroblastoma (4, 8). We recently showed that HIF2 α and insulin-like growth factor (IGF)-II are coexpressed in SNS ganglia and paraganglia during distinct periods of normal human embryogenesis and fetal development. Expression of HIF2A and IGF2 thereto correlate in clinical neuroblastoma specimens, and IGFII regulates hypoxic expression of HIF2A (12).

IGFII is a major growth factor during fetal development, whereas the related IGF1 protein primarily regulates growth during adulthood (14, 15). IGF receptor binding initiates signaling mainly through the phosphoinositide 3-kinase (PI3K) pathway (reviewed in ref. 16), which in turn regulates several important cancer hallmarks, including growth, survival, and differentiation (reviewed in ref. 17). HIF1 α translation can be regulated by growth factor–activated PI3K and mammalian target of rapamycin (mTOR) signaling (17–21). The mTOR kinase forms a complex with the cofactors and depending on whether it binds Raptor or Rictor, it forms mTORC1 or mTORC2, respectively. The PI3K/mTOR pathways are hence putative candidate mediators of IGFII-driven HIF expression and activity in neuroblastoma.

Here we show that hypoxia-induced transcription of HIF2A in neuroblastoma cell lines and cells from patient-derived xenografts (PDX) is dependent on PI3K signaling mediated by ligand-stimulated IGF1R or INSR; however, the effects appear to be independent of downstream Akt and mTORC1 activity. Abrogation of PI3K severely diminishes hypoxic HIF2 α and HIF2 target gene, including VEGF-A, expression, and results in smaller and less vascularized tumors *in vivo*. We further show that transcription of

¹Translational Cancer Research, Lund University Cancer Center at Medicon Village, Lund University, Lund, Sweden. ²Department of Medical Oncology, Molecular Oncology Laboratories, Weatherall Institute of Molecular Medicine, University of Oxford, Oxford, United Kingdom.

Note: Supplementary data for this article are available at Cancer Research Online (<http://cancerres.aacrjournals.org/>).

S. Mohlin and A. Hamidian contributed equally to this article.

Corresponding Author: Sven Pahlman, Lund University, Medicon Village, Building 406, Lund SE-22381, Sweden. Phone: 462226421; Fax: 4640337063; E-mail: sven.pahlman@med.lu.se

doi: 10.1158/0008-5472.CAN-15-0708

©2015 American Association for Cancer Research.

HIF2A is strongly dependent on mTORC2, and that PI3K and mTORC2 are potential therapeutic targets in HIF2 α -driven aggressive neuroblastomas.

Materials and Methods

Cells and reagents

The human neuroblastoma cell lines SK-N-BE(2)c, SH-SY5Y, SH-EP, IMR-32, KCN-69n (kind gifts 1979 and following years from Drs. June Biedler, Memorial Sloan Kettering Cancer Center and Robert Ross, Fordham University, Bronx, NY), and LA-N-5 (kind gift 1979 from Dr. Robert Seeger, Children's Hospital, Los Angeles, CA) were cultured in minimal essential or RPMI-1640 (IMR-32) medium. Renal cell carcinoma (RCC)-derived 786-O (ATCC) or RCC-4 (empty vector or +VHL; Sigma Aldrich) cells (used directly after purchase) were cultured in Dulbecco's Modified Eagle Medium. Genitcin (0.5 mg/mL; Gibco) was added to RCC-4 growth medium for selection. All medium was supplemented with fetal bovine serum and antibiotics. As part of our laboratory routines, neuroblastoma cell lines in use were regularly replaced on a tri-monthly basis, and screened for presence of mycoplasma infections. Morphology, growth characteristics, and critical gene expression patterns (e.g., *MYCN*, *TH*, *CHGA*) were continuously monitored by light microscopy, qRT-PCR, and Western blot. Hypoxia was generated in an InvivoO2 hypoxia workstation (Ruskin Technologies) or a Whitley H35 Hypoxystation (Don Whitley Scientific). Cells were treated with rapamycin (1 μ mol/L; Sigma Aldrich), LY294002 (50 μ mol/L; Sigma Aldrich), GDC-0941 (1 μ mol/L; Selleckchem), PI-103 (1 μ mol/L; Selleckchem), NVP-AEW540 (1 μ mol/L; Selleckchem), HNMPA-(AM)₃ (1 μ g/mL; Enzo Life Sciences), GDC-0068 (1 μ mol/L; Selleckchem); or PP242 (1 μ mol/L; Selleckchem).

Western blotting

Cells were lysed in RIPA supplemented with complete protease inhibitor and phosSTOP. Proteins were separated by SDS-PAGE and transferred to polyvinylidene difluoride or Hybond-C-Extra nitrocellulose membranes. Antibodies are listed in Supplementary Table S1.

Quantitative real-time PCR

Total RNA was extracted either manually using the RNeasy Mini Kit (Qiagen) or automatically using the Arrow with Arrow RNA (Tissue Kit-DNA Free) Kit (DiaSorin). cDNA synthesis and qRT-PCR was performed as described previously (12). Three reference genes were used to normalize gene-of-interest expression. Primer sequences are listed in Supplementary Table S2.

ELISA

ELISA plates (96-well; Peptrotech) were coated with capture antibody (0.5 μ g/ μ L). Samples were incubated with detection antibody (0.25 μ g/ μ L) followed by an avidin-horseradish peroxidase conjugate (1:2,000). ABTS liquid substrate was used to monitor color development at 405 nm with wavelength correction set at 650 nm.

Transfections

Transfections were performed in serum- and penicillin-free OPTI-MEM medium (Gibco), using siRNA targeting *IGF1R*, *IGF2R*, *INSR*, *AKT1-3*, *RAPTOR*, or a nontargeting control siRNA for 6 hours at 21% O₂. Following overnight recovery, cells were

transferred to hypoxia for indicated time points. Oligo concentrations used were 5 to 50 nmol/L with Lipofectamine 2000 (Invitrogen) as transfection reagent. RNAi oligo sequences, specified concentrations, and product details are listed in Supplementary Table S3.

SIN1 overexpression

SK-N-BE(2)c cells (2.5×10^5) were transfected with 5 μ g SIN1 full-length vector (pCMV6-MAPKAP1; RC211745, Origene) in 2 mL OPTI-MEM medium (Gibco) using Lipofectamine 3000 for 5 to 6 hours according to the manufacturer's recommendations. Cells were allowed to recover overnight before incubation at 21% O₂ for 48 hours.

Animal procedures and immunohistochemistry

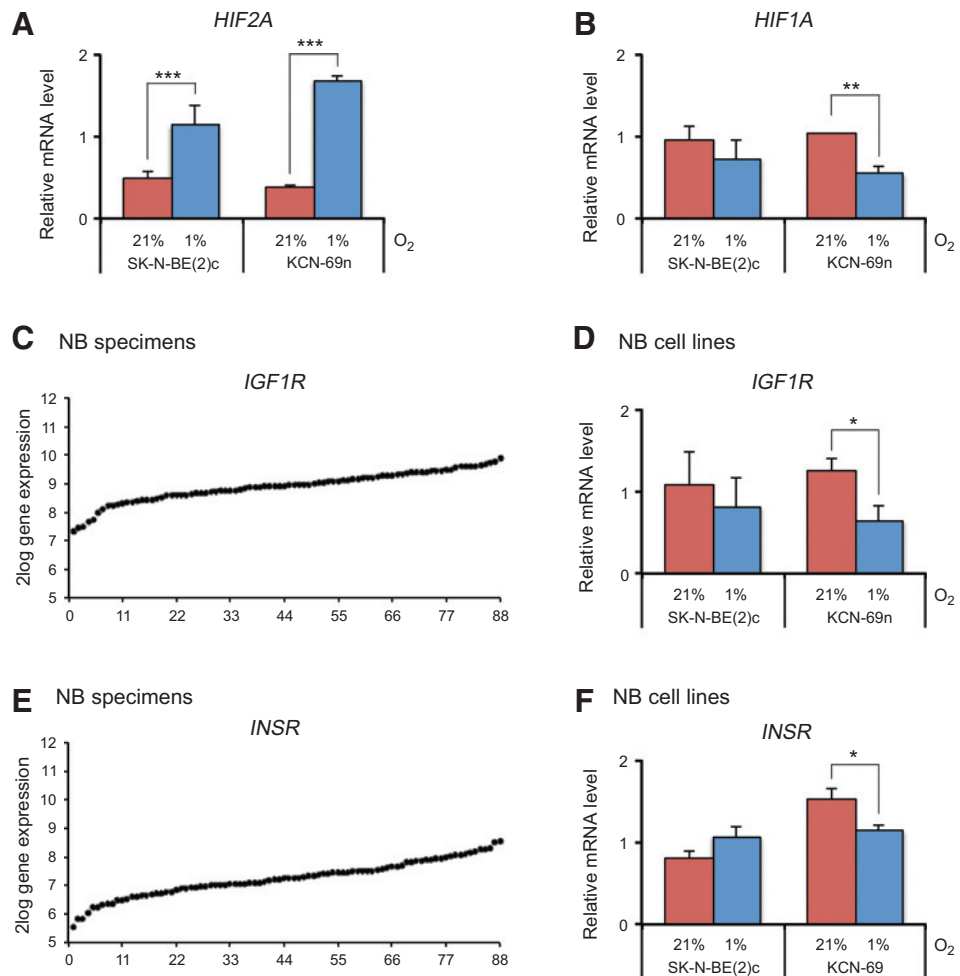
Female athymic mice (NMRI-Nu/Nu strain; Taconic) were housed in a controlled environment and the regional ethics committee for animal research approved all procedures (approval no. M69/11). SK-N-BE(2)c cells were subjected to DMSO or LY294002 treatment for 4 hours at 21% O₂ before cells (5×10^6) were collected in 100 μ L Matrigel:PBS (2,3:1) and injected into the right flank. Tumors ($n = 7$ in each group) were measured [$V = (\pi \times l \times s^2)/6 \text{ mm}^3$, where l is the long side and s is the short side] and weighed 5 days after injection before being fixed in 4% paraformaldehyde and embedded in paraffin. After antigen retrieval using PT Link (Dako), staining of sections (4 μ m) for rat anti-mouse CD34 (Santa Cruz Biotechnology, sc-18917) was performed using AutostainerPlus (Dako).

Gene expression microarray analyses

SK-N-BE(2)c cells were treated with DMSO or PP242 for 24, 48, or 72 hours at 1% oxygen. Untreated SK-N-BE(2)c cells harvested at $T = 0$ hour were used as a normoxic control. Total RNA from four independent repeats was extracted manually using the RNeasy Mini Kit (Qiagen) according to the manufacturer's instructions. RNA quality was assessed using an Agilent 2100 Bioanalyzer (Agilent). RNA samples were hybridized to Human HT-12 v4.0 Expression BeadChips (Illumina Inc.). Mean spot intensities were background corrected and quantile normalized using BioArray Software Environment (BASE; ref. 22). Normalized data were log₂ transformed, and probes were merged on official gene symbols (mean expression) using R statistical language (version 3.1.1). The hypoxia gene expression signature score was calculated as the mean expression of 44 prototypical hypoxic response genes as described by Li and colleagues (23). Gene set enrichment analysis (GSEA; ref. 24) was performed on a ranked list of all genes based on differential expression between DMSO and PP242 treatments after 72 hours using the c2.all.v4.0 curated gene set collection (25). Differential expression was determined by significance of microarrays (SAM) analysis performed in R using the samr package (version 2.0). The data discussed in this article have been deposited in NCBI's Gene Expression Omnibus and are accessible through GEO Series accession number GSE69833 (26).

PDX model

The neuroblastoma PDX model, FDG-PET scanning procedures, and *in vitro* culturing of PDX-derived cells are described in ref. 27. Dissociated cells were treated with LY294002 or PP242 at $T = 0$ and $T = 24$ hours and cultured at 21% or 1% oxygen levels for 48 hours in total.

**Figure 1.**

Neuroblastoma cells express *IGF1R* and *INSR*. A–B, *HIF2A* (A) and *HIF1A* (B) mRNA expression in SK-N-BE(2)c and KCN-69n cells cultured at normoxia (21% O₂) or hypoxia (1% O₂) for 48 hours. C–F, *IGF1R* (C–D) and *INSR* (E–F) mRNA expression in clinical neuroblastoma material consisting of 88 tumors (C and E) and in SK-N-BE(2)c and KCN-69n cells cultured at 21% or 1% O₂ for 72 hours (D and F). Relative mRNA was measured by qRT-PCR; data, mean \pm SEM from at least three independent experiments. Statistical significance was calculated using the Student *t* test: *, *P* < 0.05; **, *P* < 0.01; ***, *P* < 0.001. No asterisk indicates no significance.

Statistical analyses

All values are reported as mean \pm SEM from at least three independent experiments unless otherwise stated. The two-sided Student unpaired *t* test was used for statistical analyses, and three levels of significance were used: *, *P* < 0.05; **, *P* < 0.01; ***, *P* < 0.001. A publicly available dataset containing 88 neuroblastomas (R2: microarray analysis and visualization platform; ref. 28) was used to analyze *INSR*, *IGF1R*, and *IGF2R* expression.

Results

HIF2A expression depends on IGF1R- and INSR-mediated signaling

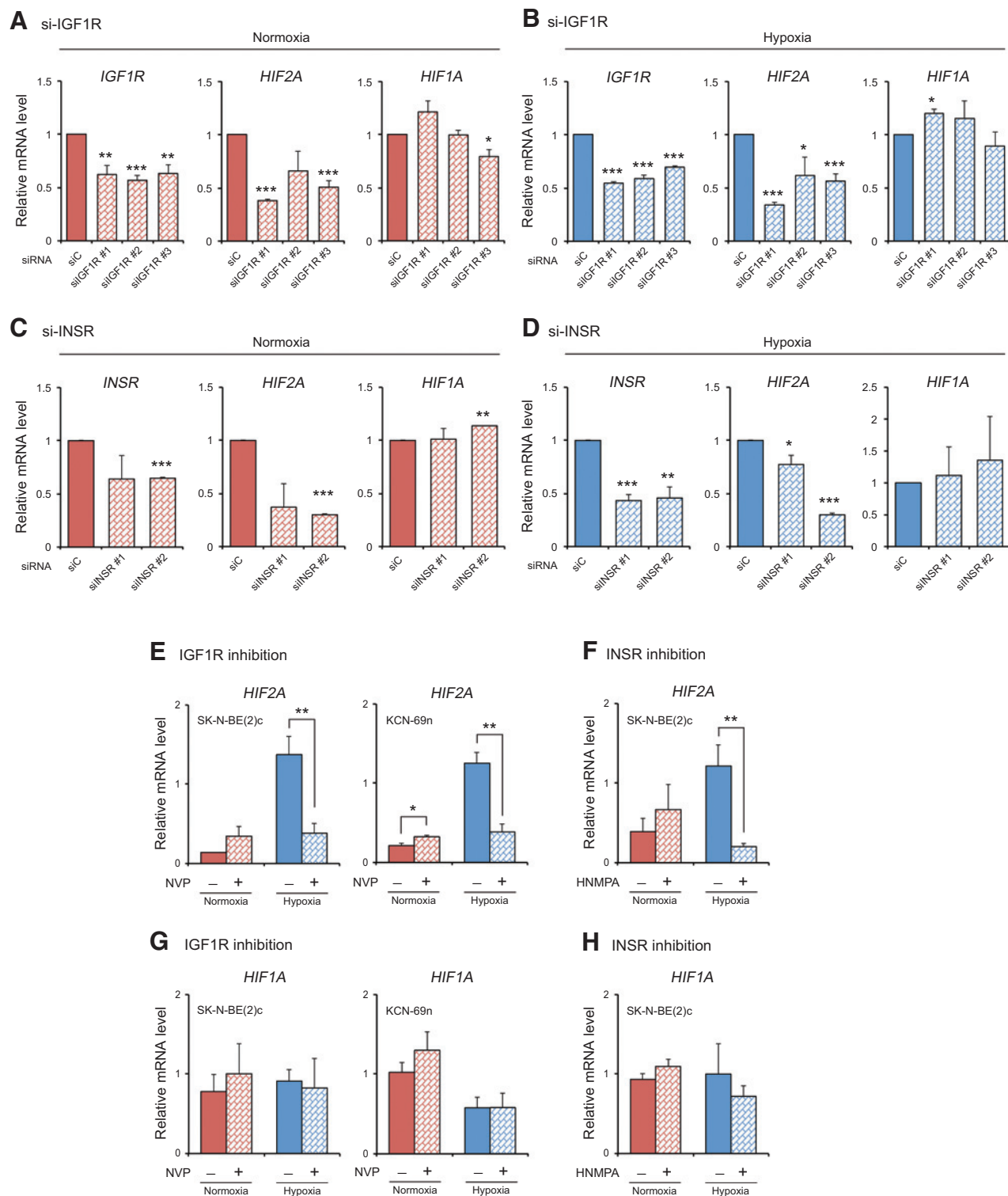
Neuroblastoma cells respond to hypoxia by differentially expressing the oxygen-sensitive HIF α subunits at protein level, with continuous accumulation of HIF2 α protein over time (4). As shown here, *HIF2A* mRNA expression mimicked HIF2 α protein expression patterns and increased with prolonged hypoxia (here defined as 1% oxygen; Fig. 1A). Because we have previously shown that IGFII regulates *HIF2A* expression (12), we analyzed expression of the receptors known to bind IGFII: *IGF1R*, *IGF2R*, and *INSR*. All three genes were expressed in neuroblastoma specimens and in SK-N-BE(2)c and KCN-69n neuroblastoma cells (Fig. 1C–F; Supplementary Fig. S1A and S1B). *IGF2R* encodes a protein devoid

of an extended intracellular tail, and the receptor is considered to lack signal transduction capacity. Consequently, downregulation of *IGF2R* expression did not affect *HIF2A* levels (Supplementary Fig. S1C and S1D).

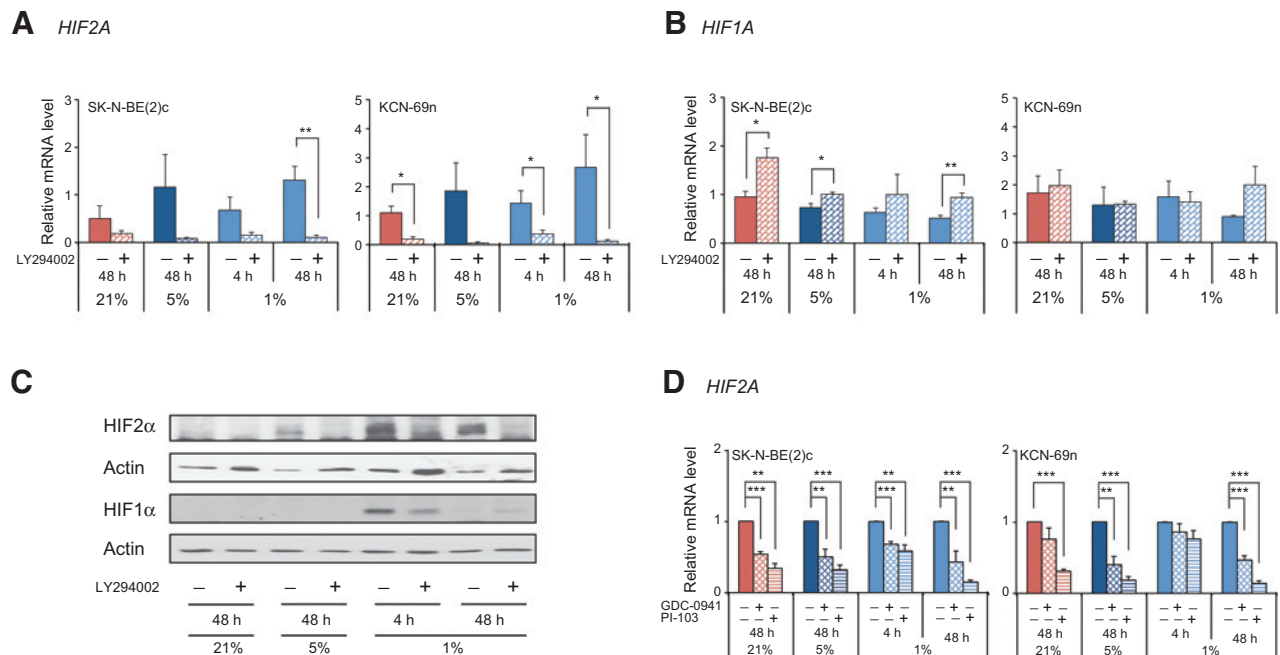
RNAi-mediated downregulation of *IGF1R* and *INSR* resulted in a substantial reduction in *HIF2A* expression (Fig. 2A–D). In addition, treatment with NVP-AEW541 or HNMPA-(AM)₃, which inhibit *IGF1R* and *INSR* kinase activities, respectively, nearly completely ablated hypoxia-induced transcription of *HIF2A* (Fig. 2E and F). The effects on *HIF1A* mRNA expression were less coherent, depending on oxygen concentrations and oligo target sequence (Fig. 2A–D and G–H). We conclude that *IGF1R* and *INSR* signaling have no unanimous effect on *HIF1A* transcription in neuroblastoma cells.

PI3K differentially regulates HIF1 α and HIF2 α protein expression

The PTEN–PI3K–AKT–mTOR pathway is implicated both in HIF translation (refs. 18, 20 and reviewed in refs. 17, 19) and in transducing signals evoked by *IGF1R* and *INSR* (reviewed in ref. 16). PI3K signaling is not generally hyperactivated by PTEN or PIK3CA deletions or mutations in neuroblastoma (29, 30), and, as shown in Supplementary Fig. S2A, PTEN protein was expressed in all the neuroblastoma cell lines studied. Hypoxia

**Figure 2.**

HIF2A transcription is dependent on functional IGF1R and INSR. A–D, expression of *HIF2A* and *HIF1A* mRNA after downregulation of *IGF1R* (A–B) and *INSR* (C–D) in SK-N-BE(2)c cells using siRNAs under normoxia (21% O₂; A and C) or hypoxia (1% O₂; B and D). Expression was normalized against siC within each experiment, and statistical significance was calculated compared with siC. E–H, expression of *HIF2A* and *HIF1A* mRNA after treatment with the IGF1R inhibitor NVP-AEW541 (E and G) or the INSR inhibitor HNMPA-(AM)₃ (F and H) for 48 hours, as measured by qRT-PCR. Data, mean ± SEM from three independent experiments. Statistical significance was calculated using the Student *t* test: *, *P* < 0.05; **, *P* < 0.01; ***, *P* < 0.001. No asterisk indicates no significance.

**Figure 3.**

PI3K signaling is required for *HIF2A* expression. A and B, cells were treated with the PI3K inhibitor LY294002 for 4 or 48 hours at 21%, 5%, or 1% O₂ and *HIF2A* (A) and *HIF1A* (B) mRNA was quantified. C, HIF1 α and HIF2 α protein levels were determined by Western blotting after treatment of KCN-69n cells with LY294002 for 4 or 48 hours at 21%, 5%, or 1% O₂. Actin was used as loading control. D, cells were treated with PI3K inhibitors GDC-0941 or PI-103 for 4 or 48 hours at 21%, 5%, or 1% O₂ and *HIF2A* mRNA measured. Expression was normalized against control within each setting. mRNA levels were quantified by qRT-PCR; data, mean \pm SEM from three independent experiments. Statistical significance was calculated using the Student *t* test: *, *P* < 0.05; **, *P* < 0.01; ***, *P* < 0.001. No asterisk indicates no significance.

resulted in an increase in phosphorylated Akt (at Ser473), indicating persistent hypoxia-driven activation of the PI3K pathway (Supplementary Fig. S2B). Pharmacologic inhibition of PI3K activity with LY294002 nearly eradicated *HIF2A* mRNA expression (Fig. 3A), whereas *HIF1A* expression was unaffected or even slightly upregulated (Fig. 3B). HIF2 α protein expression was abolished, whereas acute hypoxic induction of HIF1 α was partly prevented by LY294002 (Fig. 3C). To account for off-target effects of LY294002, two additional PI3K inhibitors (GDC-0941 and PI-103) were examined. Both inhibitors significantly downregulated *HIF2A* mRNA expression (Fig. 3D).

PI3K inhibition affects HIF2-regulated gene expression and *in vivo* tumor growth

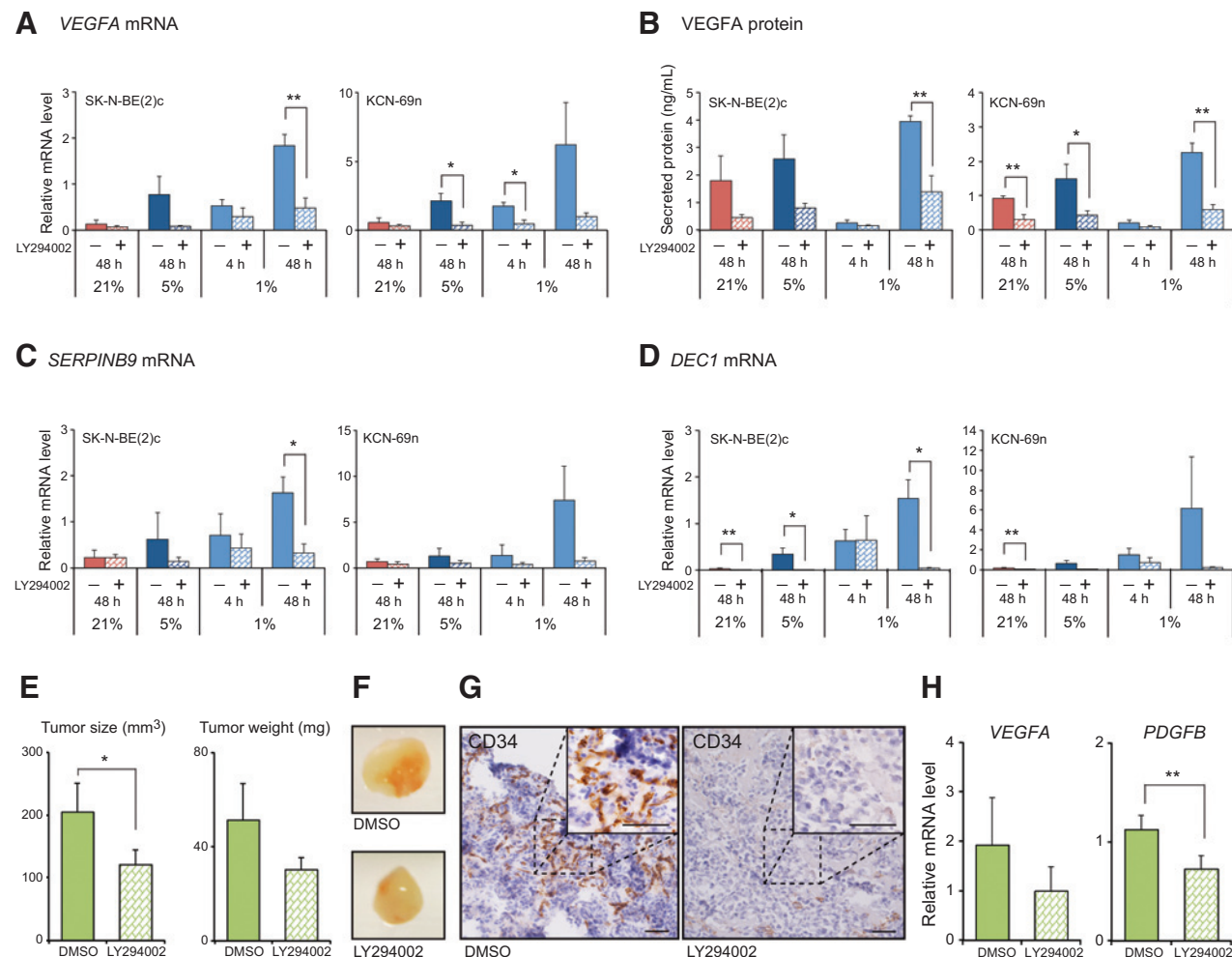
To determine if *HIF2A* downregulation by PI3K inhibition has biologic consequences, expression of known HIF2-driven genes in neuroblastoma (such as *VEGFA*, *SERPINB9*, and *DEC1*; ref. 4) was measured. VEGF-A mRNA and protein expression was induced under physiologic and long-term hypoxic oxygen tensions, conditions under which HIF2 α protein is the dominant HIF α subunit (Figs. 3C and 4A and B). When PI3K activity, and hence HIF2 α expression, was blocked, VEGF-A protein and mRNA levels (Fig. 4A and B) and *SERPINB9* and *DEC1* mRNA levels (Fig. 4C and D) were drastically reduced.

A variety of extracellular stimuli are transduced by PI3K. In an attempt to investigate the *in vivo* effects of PI3K inhibition on tumor growth and vascularization without affecting systemic PI3K signaling, SK-N-BE(2)c cells were pretreated with LY294002 prior to subcutaneous injection into mice. After a short period of

tumor growth (5 days), mice were sacrificed. Compared with vehicle controls, the size and weight of tumors were negatively affected by LY294002 (Fig. 4E). Tumors derived from LY294002-treated cells were considerably less vascularized (Fig. 4F and G) and expressed lower mRNA levels of the pro-angiogenic growth factors *VEGFA* and *PDGFB* (Fig. 4H).

PI3K affects HIF2A mRNA expression independently of Akt

Akt is classically considered the most common mediator of PI3K signaling, and neuroblastoma cells expressed all three AKT genes (Supplementary Fig. S3A–S3C). GDC-0068 is a highly selective pan-Akt inhibitor that is currently in clinical trials (31). Inhibiting Akt using GDC-0068 had no effect on *HIF2A* or *HIF1A* mRNA expression, either with short-term (1 hour; Supplementary Fig. S3E) or long-term (48 hours; Fig. 5A) treatment. To verify inhibitor efficacy, we examined the expression of phosphorylated PRAS40, a downstream target of Akt. PRAS40 (pT246) levels were only slightly decreased (Supplementary Fig. S3F and S3G); however, the effect of GDC-0068 treatment on PRAS40 has been reported to vary between cell lines and tissue types (31). Because GDC-0068 is an ATP-competitive inhibitor, pAkt levels increase despite decreased downstream signaling (31). As expected, we observed inhibitor-dependent pAkt (S473) upregulation at all time points and oxygen tensions (Supplementary Fig. S3H). We next knocked down Akt using siRNAs. Combined elimination of the three Akt variants had no effect on *HIF2A* mRNA levels (Fig. 5B), despite high knockdown efficiency (Supplementary Fig. S3D). PI3K can exert its effects via several distinct pathways (e.g., BMX/ETK,

**Figure 4.**

Inhibiting PI3K activity abrogates the biologic activity of HIF2 α . A–D, cells were treated with LY294002 for 4 or 48 hours at 21%, 5%, or 1% O₂ and VEGFA mRNA (A), VEGFA protein (B), and SERPINB9 (C) or DEC1 (D) mRNA levels were measured by qRT-PCR (mRNA) or ELISA (secreted protein). Data, mean \pm SEM from three independent experiments. E–H, LY294002 or vehicle pretreated SK-N-BE(2)c cells were injected subcutaneously into nude mice. E, tumor size and weight after 5 days of tumor growth ($n = 5$ in each group). F, representative images of tumors formed from DMSO- or LY294002-treated cells. G, immunohistochemical staining for murine CD34. Scale bars, 100 μ m. H, qRT-PCR analysis of VEGFA and PDGFB mRNA. Data, mean \pm SEM ($n = 5$ in each group). Statistical significance was calculated using the Student t test: *, $P < 0.05$; **, $P < 0.01$. No asterisk indicates no significance.

S6K1, PDPK1, and SGK3; ref. 32, and reviewed in ref. 33), but we could not attribute PI3K-dependent HIF2 α /HIF1 α expression to any of these signal transducers based on knockdown studies.

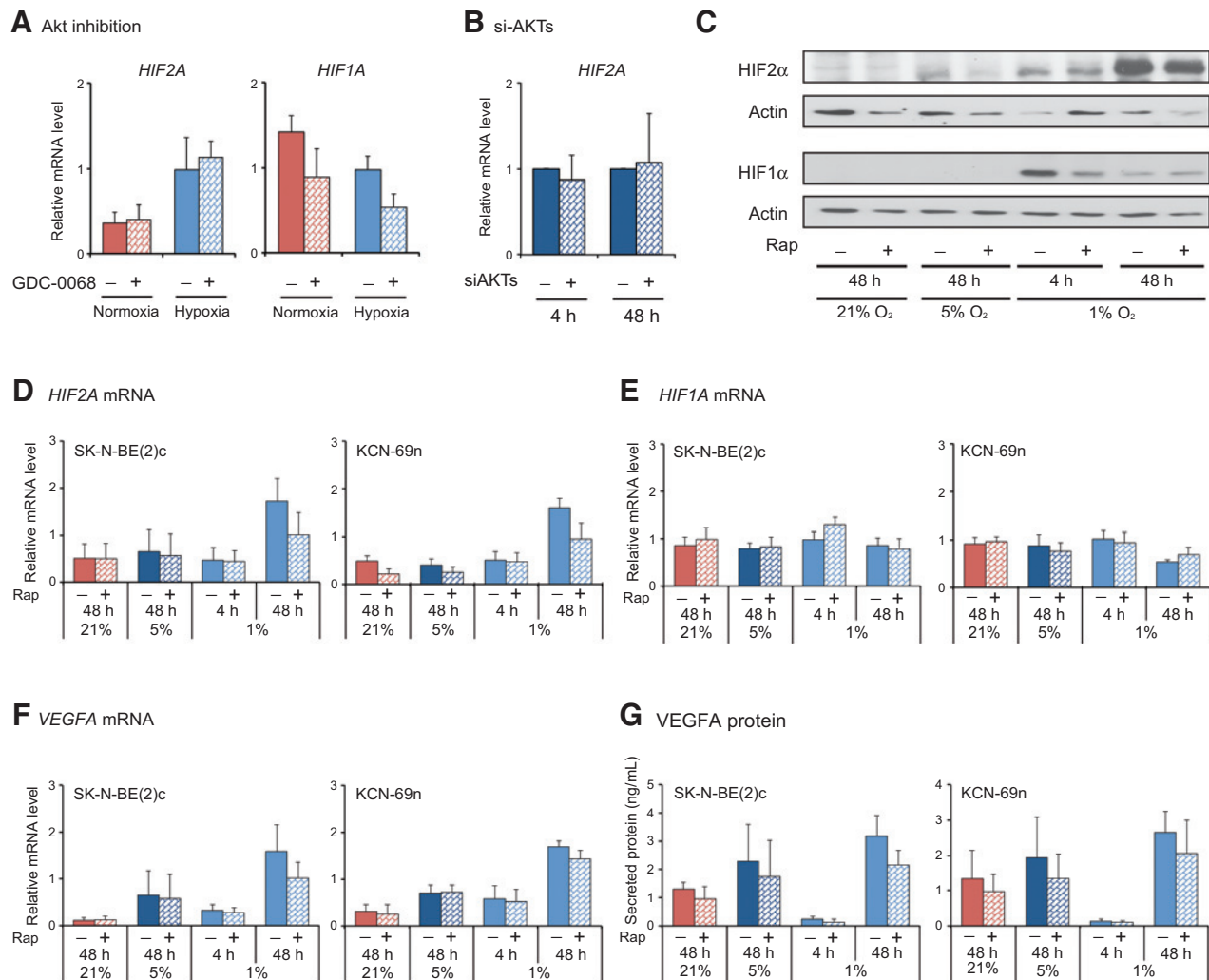
mTORC1 regulates HIF1 α protein translation only

Because mTORC1 has been implicated in HIF regulation, we knocked down expression of the mTORC1-specific protein Raptor. This had no effect on HIF2A mRNA levels (Supplementary Fig. S3I). In addition, neuroblastoma cells were treated with rapamycin, a compound that inhibits mTORC1 by binding to, and thereby interrupting, the kinase of the complex (reviewed in ref. 34). HIF2 α protein expression was virtually unaffected, whereas HIF1 α protein levels were downregulated at acute hypoxia (Fig. 5C). Rapamycin treatment had no significant effect on HIF2A or HIF1A transcription (Fig. 5D and E), the HIF2-driven genes VEGFA, DEC1 or SERPINB9, or hypoxia-induced VEGFA

protein expression (Figs. 5F and G; Supplementary Fig. S4A and S4B).

PI3K-mediated regulation of HIF2A is exerted via mTORC2

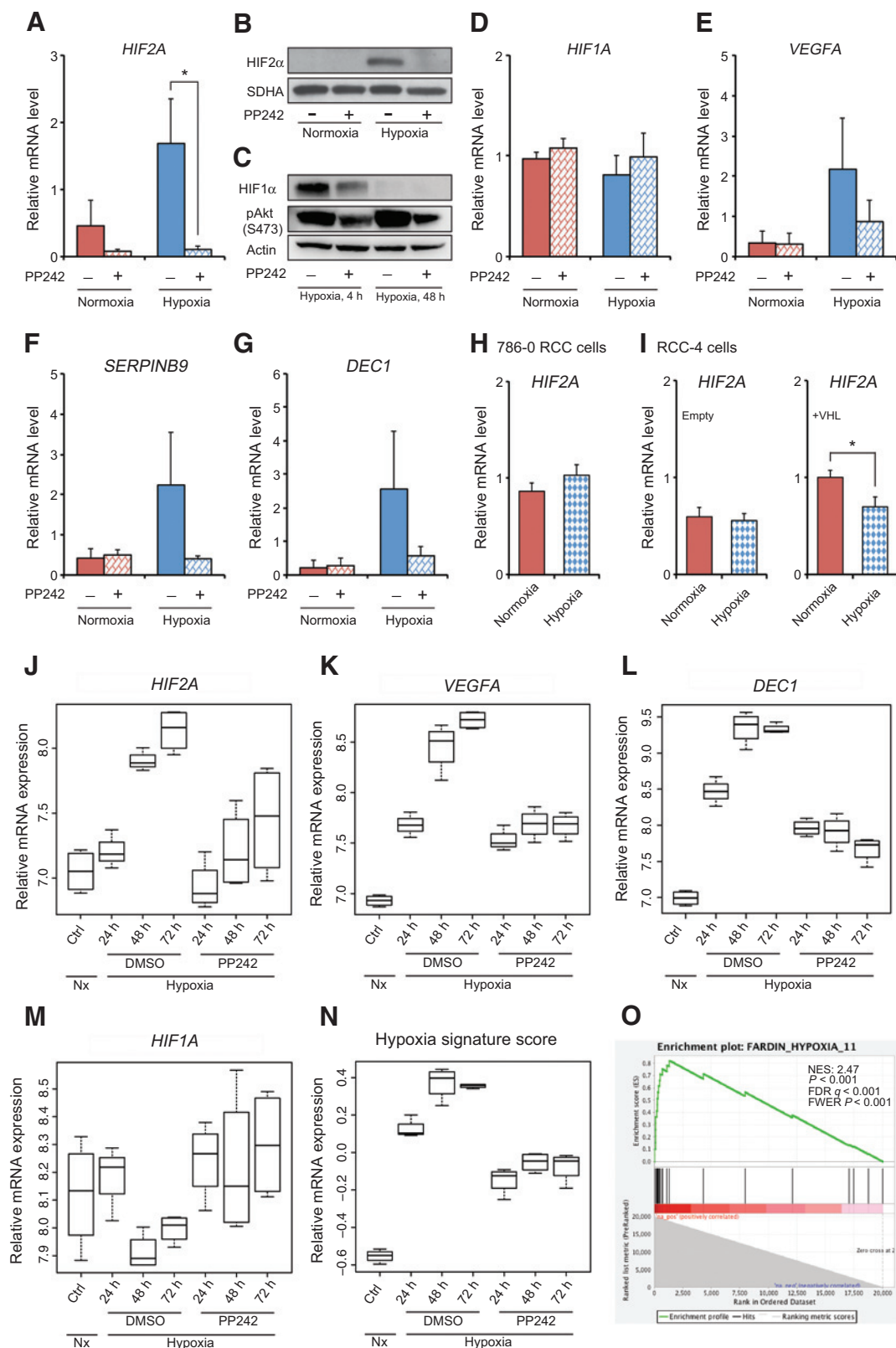
HIF2 α protein levels can be regulated via mTORC2 in 786-O and RCC4 clear cell RCC cells (20, 35). Prolonged treatment of SK-N-BE(2)c neuroblastoma cells with the mTORC1/mTORC2 inhibitor PP242 virtually eradicated HIF2 α mRNA and protein expression (Fig. 6A and B). Consistent with rapamycin data, HIF1 α protein expression was partly downregulated after 4 hours of treatment (Figs. 5C and 6C). Akt is phosphorylated at Ser473 by mTORC2, which hence serves as a surrogate marker of mTORC2 activity. PP242 treatment robustly dampened pAkt (S473) expression under both short-term and long-term conditions (Fig. 6C). Despite reduced HIF1 α protein expression following PP242 treatment, HIF1A mRNA was unaffected (Fig. 6D); however, hypoxia-induced expression of HIF2

**Figure 5.**

Akt and mTORC1 signaling is dispensable for transcription of *HIF2A*. A, SK-N-BE(2)c cells were treated with the Akt inhibitor GDC-0068 for 48 hours at normoxia (21% O₂) or hypoxia (1% O₂), and mRNA levels of *HIF2A* and *HIF1A* were determined using qRT-PCR. B, *HIF2A* expression after combined knockdown of all three AKT isoforms for 4 or 48 hours at 5% O₂. Expression was normalized against control. C, HIF2 α and HIF1 α protein levels were determined by Western blotting after treatment of KCN-69n cells with the mTORC1 inhibitor rapamycin for 4 or 48 hours at 21%, 5%, or 1% O₂. Actin was used as loading control. D–G, cells were treated with rapamycin for 4 or 48 hours at 21%, 5%, or 1% O₂ and *HIF2A* (D), *HIF1A* (E), and *VEGFA* (F) mRNA and VEGF-A protein (G) levels were quantified using qRT-PCR (mRNA) or ELISA (secreted protein). Data, mean \pm SEM from three independent experiments. Statistical significance was calculated using the Student *t* test. No asterisk indicates no significance.

target genes *VEGFA*, *SERPINB9*, and *DEC1* was markedly reduced in PP242-treated cells (Fig. 6E–G). Because this differential dependence of HIF1 α and HIF2 α on mTORC1 and mTORC2 has also been reported in RCC (20, 35), we sought to establish if *HIF2A* is transcriptionally regulated in RCC-derived cells. However, there was no significant hypoxic induction of *HIF2A* mRNA expression in either 786-O or RCC-4 cells (Fig. 6H and I), indicating that transcriptional regulation of *HIF2A* might be cell-type dependent. RCC cell lines 786-O and RCC-4 lack, or have mutant, expression of the von Hippel Lindau (VHL) gene. Because the VHL protein targets HIF α subunits for ubiquitination and degradation at normoxia, RCC-4 cells stably transduced with a VHL-containing vector were analyzed. As shown in Fig. 6I, restored VHL expression rather decreased *HIF2A* transcription at hypoxia.

In order to further validate the effects of PP242 on HIF activation, we performed gene expression microarray analysis of SK-N-BE(2)c cells treated with PP242 at hypoxia for 24, 48, or 72 hours. As above, PP242 inhibited the hypoxic induction of *HIF2A* (Fig. 6J) but not *HIF1A* (Fig. 6M). Of note, the HIF target genes *VEGFA* and *DEC1* also had reduced hypoxic induction (Fig. 6K and L), which was most prominent at later time points (48 and 72 hours), implying that the early hypoxic response (over the first 24 hours) is not substantially affected by PP242 treatment. In addition, a transcriptional signature of hypoxic pathway activity (23) was also reduced at later time points following PP242 treatment (Fig. 6N), and GSEA of genes ranked according to differential expression between 72-hour treatments with DMSO and PP242 displayed significant enrichment for genes involved in the hypoxic response (Fig. 6O).

**Figure 6.**

HIF2A transcription depends on mTORC2 activity. A–B, SK-N-BE(2)c cells were treated with the dual mTORC1/mTORC2 inhibitor PP242 for 48 hours at normoxia (21% O₂) or hypoxia (1% O₂), and *HIF2A* mRNA (A) or *HIF2A* protein (B) was measured by qRT-PCR (mRNA) or Western blotting (protein). (Continued on the following page.)

The mTORC2 complex consists of several distinct proteins. Because *HIF2A* expression is reduced by mTORC2 inhibition, we overexpressed SIN1, an mTORC2-specific component. SIN1 overexpression, and presumably increased mTORC2 activity, led to significant increase in *HIF2A* transcription in neuroblastoma cells (Fig. 7A).

HIF2A mRNA expression is regulated by PI3K in neuroblastoma PDX-derived cells

We recently reported a PDX model of neuroblastoma in which patient tumor tissue is orthotopically implanted into mice. Resulting tumors closely resemble clinical neuroblastomas with widespread metastasis, including to bone marrow (Fig. 7B; ref. 27). Tumors growing in mice were resected, dissected, and grown in stem cell-promoting medium to allow the cells to grow as neurospheres (27). Importantly, these cells demonstrated hypoxia-induced *HIF2A* mRNA expression (Fig. 7C), similar to the classical SK-N-BE(2)c and KCN-69n neuroblastoma cell lines (Fig. 1A). Treatment of the PDX-derived cells with LY294002 or PP242 under hypoxic conditions resulted in downregulated *HIF2A* mRNA expression (Fig. 7C), further supporting a role for PI3K and mTORC2 signaling in regulating HIF2 in human neuroblastomas.

Discussion

Because high HIF2 α , but not HIF1 α , protein expression is associated with aggressive disease in neuroblastomas and several other tumor types, identification of the pathways that specifically regulate the expression and activity of different HIF α subunits may provide novel avenues for therapeutic intervention. Unlike canonical HIF posttranslational regulation, we show here that the hypoxia-induced increase in HIF2 α protein expression in neuroblastoma cells is, to a large extent, explained by transcriptional upregulation of *HIF2A*. Interestingly, this mode of regulation mimics the situation during normal SNS development where HIF2 α protein is transcriptionally regulated in immature neuroblasts and paraganglia cells (12, 36).

PI3K and/or mTOR inhibition severely attenuates neuroblastoma cell growth *in vitro* and *in vivo* (37–39). Here, treatment with PI3K inhibitors diminishes basal- and hypoxia-induced *HIF2A* expression. In addition, neuroblastoma cells pretreated with the PI3K inhibitor LY294002 formed smaller and less vascularized tumors *in vivo*. The results are in agreement with previous findings where *HIF2A* knockdown in neuroblastoma cells gave rise to smaller and more slow-growing tumors (4), and where high HIF2 α levels were detected in well-vascularized tumor regions, whereas HIF1 α expression significantly correlated negatively with vascularization in human neuroblastoma (4, 8).

Having established that PI3K inhibition strongly reduced HIF2-dependent gene transcription and tumor growth, we searched for

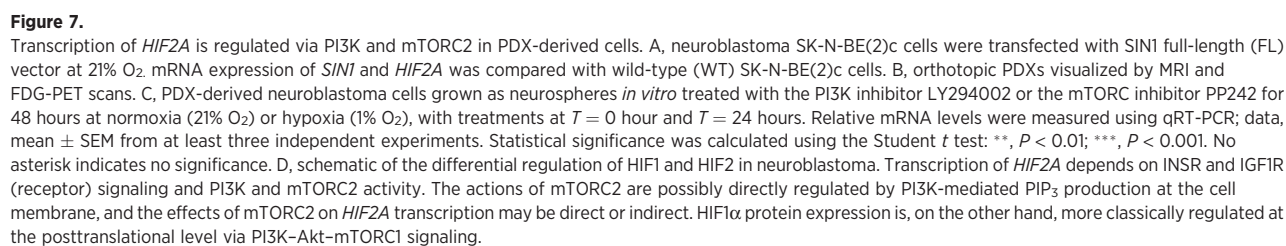
downstream regulatory events that might be more efficiently targeted. Neither gene knockdown nor inhibition of Akt activity affected *HIF2A* expression. Although PI3K primarily relays its activity via Akt, there are previous demonstrations of Akt-independent PI3K signaling in human tumors (40, 41). We conclude that PI3K regulates HIF2 α via Akt- and mTORC1-independent mechanisms.

Little is known about upstream and downstream effects of mTORC2, but it has been suggested to be directly or indirectly activated by PI3K (42–46). VHL-deficient RCC cells that constitutively express HIF2 α have been shown to have differential dependency on mTORC1 and mTORC2 for HIF1 α and HIF2 α protein expression (20). We confirm these results in neuroblastoma. However, this effect is mediated by transcriptional downregulation of *HIF2A*, highlighting a fundamental difference between the actions of mTORC1 on HIF1 and mTORC2 on HIF2 activities, respectively.

We have recently generated neuroblastoma PDXs (27) by orthotopic implantation of tumor explants from high-risk neuroblastoma patients into immunocompromised mice. The resulting tumors closely resemble clinical neuroblastomas, with widespread metastasis to clinically relevant sites. Compared with classical cell lines grown *in vitro* for decades that display genotypic and phenotypic alterations, neuroblastoma PDXs retain the characteristics of the tumors from which they were derived (27). In addition, *in vitro*-cultured neuroblastoma PDX-derived cells retain their tumorigenic and metastatic capacity upon orthotopic injection into mice (27). PDX-based tumor models are increasingly being used in cancer research for drug screening and testing of novel therapeutic targets due to being more predictive of clinical outcome than cell line-derived xenografts (47). Here, we demonstrate the feasibility of using short-term *in vitro* cultured neuroblastoma PDX-derived cells as a drug-testing model and show that *HIF2A* mRNA expression is regulated by hypoxia via the PI3K/mTORC2 pathway in these cells. Compared with treatment of classical neuroblastoma cell lines with PI3K and mTOR inhibitors, the *HIF2A* effects in PDX-derived cells were significant but somewhat modest (Fig. 7B). These results may, however, be explained by low drug penetrance into PDX-derived neurospheres compared with monolayer cultures (unpublished observations).

In summary, IGFII-driven *HIF2A* mRNA expression in hypoxic neuroblastoma cells is executed via IGF1R/INSR-PI3K-mTORC2 signaling, whereas HIF1 α is regulated only at the protein level via PI3K-mTORC1 (Fig. 7D). Because *HIF2A* expression seems to require both IGF1R and INSR, it is tempting to speculate that the subunits of these receptors form hybrid receptor complexes upon IGFII ligand binding to exclusively direct signaling via the PI3K-mTORC2 axis when hypoxic. Although we have not addressed whether the changes in *HIF2A* mRNA expression are due to mRNA stability or *de novo* transcription, it has been reported that HIF mRNA expression in hypoxic neuroblastoma cells is controlled by

(Continued.) SDHA was used as loading control. C, HIF1 α and pAkt(S473) protein levels were determined by Western blotting after treatment of hypoxic SK-N-BE(2)c cells with PP242 for 4 or 48 hours. Actin was used as loading control. D–G, normoxic or hypoxic SK-N-BE(2)c cells were treated with PP242 for 48 hours and *HIF1A* (D), *VEGFA* (E), *SERPINB9* (F), and *DEC1* (G) mRNA was measured. H–I, *HIF2A* mRNA levels in RCC-derived 786-O (H) or RCC-4 (I) cells cultured at normoxia or hypoxia for 48 hours. Relative mRNA levels were determined using qRT-PCR and data are mean \pm SEM from three independent experiments. Statistical significance was calculated using the Student *t* test: **P* < 0.05. No asterisk indicates no significance. J–M, *HIF2A* (J), *VEGFA* (K), *DEC1* (L), and *HIF1A* (M) mRNA expression obtained from gene expression microarray analysis. N, measure of hypoxic pathway activity. Expression analysis was carried out on hypoxic SK-N-BE(2)c cells cultured for 24, 48, or 72 hours and treated with DMSO or PP242. Nx, normoxia (21% O₂). O, GSEA of genes ranked according to differential expression between 72-hour treatments with DMSO or PP242 from the gene expression microarray described in J–N. NES, normalized enrichment score; FDR, false discovery rate; FWER, familywise error rate/Bonferroni correction.



transcription rather than stabilization (48). These results and our earlier findings (4, 12, 13, 49) suggest that HIF2 α inhibition, either directly or via the signaling pathways that activate HIF2 α transcription and translation, is an attractive target for the treatment of aggressive neuroblastoma. Because the PI3K pathway appears to be a major activator of HIF2 activity and PI3K/mTOR inhibitors are in clinical use and late clinical trials (reviewed in ref. 50), it is plausible that the effects of these inhibitors include inhibition of HIF2 transcription and may be particularly useful drugs for patients with neuroblastoma.

Disclosure of Potential Conflicts of Interest

No potential conflicts of interest were disclosed.

Authors' Contributions

Conception and design: S. Mohlin, A. Hamidian, K. von Stedingk, E. Bridges, S. Pahlman

Development of methodology: S. Mohlin, A. Hamidian, E. Bridges, S. Pahlman
Acquisition of data (provided animals, acquired and managed patients, provided facilities, etc.): S. Mohlin, A. Hamidian, K. von Stedingk, E. Bridges, C. Wigerup, D. Bexell, S. Pahlman

Analysis and interpretation of data (e.g., statistical analysis, biostatistics, computational analysis): S. Mohlin, A. Hamidian, K. von Stedingk, E. Bridges, C. Wigerup, D. Bexell, S. Pahlman

Writing, review, and/or revision of the manuscript: S. Mohlin, A. Hamidian, K. von Stedingk, E. Bridges, S. Pahlman

Administrative, technical, or material support (i.e., reporting or organizing data, constructing databases): S. Mohlin, A. Hamidian, K. von Stedingk, S. Pahlman

Study supervision: S. Pahlman

Acknowledgments

Lund University Bioimaging Center (LBIC), Lund University, is gratefully acknowledged for providing experimental resources.

Grant Support

This work was supported by the Swedish Cancer Society, the Children's Cancer Foundation of Sweden, the Swedish Research Council, Fru Berta Kamprads stiftelse, the SSF Strategic Center for Translational Cancer Research—CREATE Health, VINNOVA, BioCARE, a Strategic Research Program at Lund University, Hans von Kantzows Stiftelse, Gunnar Nilsson's Cancer Foundation, and the research funds of Malmö University Hospital.

The costs of publication of this article were defrayed in part by the payment of page charges. This article must therefore be hereby marked *advertisement* in accordance with 18 U.S.C. Section 1734 solely to indicate this fact.

Received March 16, 2015; revised July 27, 2015; accepted August 3, 2015; published OnlineFirst October 2, 2015.

References

- Huang LE, Gu J, Schau M, Bunn HF. Regulation of hypoxia-inducible factor 1 α is mediated by an O₂-dependent degradation domain via the ubiquitin-proteasome pathway. *Proc Natl Acad Sci U S A* 1998;95:7987–92.
- Kallio PJ, Wilson WJ, O'Brien S, Makino Y, Poellinger L. Regulation of the hypoxia-inducible transcription factor 1 α by the ubiquitin-proteasome pathway. *J Biol Chem* 1999;274:6519–25.
- Giatromanolaki A, Koukourakis MI, Sivridis E, Turley H, Talks K, Pezzella F, et al. Relation of hypoxia inducible factor 1 α and 2 α in operable non-small cell lung cancer to angiogenic/molecular profile of tumours and survival. *Br J Cancer* 2001;85:881–90.
- Holmquist-Mengelbier L, Fredlund E, Löfstedt T, Noguera R, Navarro S, Nilsson H, et al. Recruitment of HIF-1 α and HIF-2 α to common target genes is differentially regulated in neuroblastoma: HIF-2 α promotes an aggressive phenotype. *Cancer Cell* 2006;10:413–23.
- Helczynska K, Larsson AM, Holmquist Mengelbier L, Bridges E, Fredlund E, Borgquist S, et al. Hypoxia-inducible factor-2 α correlates to distant recurrence and poor outcome in invasive breast cancer. *Cancer Res* 2008;68:9212–20.
- Kronblad A, Jirstrom K, Ryden L, Nordenskjöld B, Landberg G. Hypoxia inducible factor-1 α is a prognostic marker in premenopausal patients with intermediate to highly differentiated breast cancer but not a predictive marker for tamoxifen response. *Int J Cancer* 2006;118:2609–16.
- Li Z, Bao S, Wu Q, Wang H, Eyler C, Sathornsumetee S, et al. Hypoxia-inducible factors regulate tumorigenic capacity of glioma stem cells. *Cancer Cell* 2009;15:501–13.
- Noguera R, Fredlund E, Piqueras M, Pietras A, Beckman S, Navarro S, et al. HIF-1 α and HIF-2 α are differentially regulated in vivo in neuroblastoma: high HIF-1 α correlates negatively to advanced clinical stage and tumor vascularization. *Clin Cancer Res* 2009;15:7130–6.
- Schindl M, Schoppmann SF, Samonigg H, Hausmaninger H, Kwasny W, Gnant M, et al. Overexpression of hypoxia-inducible factor 1 α is associated with an unfavorable prognosis in lymph node-positive breast cancer. *Clin Cancer Res* 2002;8:1831–7.
- Heddeston JM, Li Z, McLendon RE, Hjelmeland AB, Rich JN. The hypoxic microenvironment maintains glioblastoma stem cells and promotes reprogramming towards a cancer stem cell phenotype. *Cell Cycle* 2009;8:3274–84.
- Kim WY, Perera S, Zhou B, Carretero J, Yeh JJ, Heathcote SA, et al. HIF2 α cooperates with RAS to promote lung tumorigenesis in mice. *J Clin Invest* 2009;119:2160–70.
- Mohlin S, Hamidian A, Pahlman S. HIF2A and IGF2 expression correlates in human neuroblastoma cells and normal immature sympathetic neuroblasts. *Neoplasia* 2013;15:328–34.
- Pietras A, Gisselsson D, Öra I, Noguera R, Beckman S, Navarro S, et al. High levels of HIF-2 α highlight an immature neural crest-like neuroblastoma cell cohort located in a perivascular niche. *J Pathol* 2008;214:482–8.
- Baker J, Liu JP, Robertson EJ, Efstratiadis A. Role of insulin-like growth factors in embryonic and postnatal growth. *Cell* 1993;75:73–82.
- DeChiara TM, Efstratiadis A, Robertson EJ. A growth-deficiency phenotype in heterozygous mice carrying an insulin-like growth factor II gene disrupted by targeting. *Nature* 1990;345:78–80.
- Pollak M. Insulin and insulin-like growth factor signalling in neoplasia. *Nat Rev Cancer* 2008;8:915–28.
- Liu P, Cheng H, Roberts TM, Zhao JJ. Targeting the phosphoinositide 3-kinase pathway in cancer. *Nat Rev Drug Discov* 2009;8:627–44.
- Beppu K, Nakamura K, Linehan WM, Rapisarda A, Thiele CJ. Topotecan blocks hypoxia-inducible factor-1 α and vascular endothelial growth factor expression induced by insulin-like growth factor-I in neuroblastoma cells. *Cancer Res* 2005;65:4775–81.
- Jiang BH, Liu LZ. PI3K/PTEN signaling in angiogenesis and tumorigenesis. *Adv Cancer Res* 2009;102:19–65.
- Toschi A, Lee E, Gadir N, Ohh M, Foster DA. Differential dependence of hypoxia-inducible factors 1 α and 2 α on mTORC1 and mTORC2. *J Biol Chem* 2008;283:34495–9.
- Zhong H, Chiles K, Feldser D, Laughner E, Hanrahan C, Georgescu MM, et al. Modulation of hypoxia-inducible factor 1 α expression by the epidermal growth factor/phosphatidylinositol 3-kinase/PTEN/AKT/FRAP pathway in human prostate cancer cells: implications for tumor angiogenesis and therapeutics. *Cancer Res* 2000;60:1541–5.
- Vallon-Christersson J, Nordborg N, Svensson M, Hakkinen J. BASE-2nd generation software for microarray data management and analysis. *BMC Bioinformatics* 2009;10:330.
- Li B, Qiu B, Lee DS, Walton ZE, Ochocki JD, Mathew LK, et al. Fructose-1,6-bisphosphatase opposes renal carcinoma progression. *Nature* 2014;513:251–5.
- Subramanian A, Tamayo P, Mootha VK, Mukherjee S, Ebert BL, Gillette MA, et al. Gene set enrichment analysis: a knowledge-based approach for interpreting genome-wide expression profiles. *Proc Natl Acad Sci U S A* 2005;102:15545–50.

25. Broad Institute [Internet]. [cited 2015 Aug 20]. Available from: www.broad.mit.edu/gsea/msigdb
26. National Center for Biotechnology Information [Internet]. [cited 2015 Aug 20]. Available from: <http://www.ncbi.nlm.nih.gov/geo/query/acc.cgi?acc=GSE69833>
27. Braekeveldt N, Wigerup C, Gisselsson D, Mohlin S, Merselius M, Beckman S, et al. Neuroblastoma patient-derived orthotopic xenografts retain metastatic patterns and geno- and phenotypes of patient tumours. *Int J Cancer* 2015;136:E252–61.
28. AMC Oncogenomics [Internet]. [cited 2015 Aug 20]. Available from: <http://r2.amc.nl>
29. Dam V, Morgan BT, Mazanek P, Hogarty MD. Mutations in PIK3CA are infrequent in neuroblastoma. *BMC Cancer* 2006;6:177.
30. Moritake H, Horii Y, Kuroda H, Sugimoto T. Analysis of PTEN/MMAC1 alteration in neuroblastoma. *Cancer Genet Cytogenet* 2001;125:151–5.
31. Lin J, Sampath D, Nannini MA, Lee BB, Degtyarev M, Oeh J, et al. Targeting activated Akt with GDC-0068, a novel selective Akt inhibitor that is efficacious in multiple tumor models. *Clin Cancer Res* 2013;19:1760–72.
32. August A, Sadra A, Dupont B, Hanafusa H. Src-induced activation of inducible T cell kinase (ITK) requires phosphatidylinositol 3-kinase activity and the Pleckstrin homology domain of inducible T cell kinase. *Proc Natl Acad Sci U S A* 1997;94:11227–32.
33. Cully M, You H, Levine AJ, Mak TW. Beyond PTEN mutations: the PI3K pathway as an integrator of multiple inputs during tumorigenesis. *Nat Rev Cancer* 2006;6:184–92.
34. Benjamin D, Colombi M, Moroni C, Hall MN. Rapamycin passes the torch: a new generation of mTOR inhibitors. *Nat Rev Drug Discov* 2011;10:868–80.
35. Nayak BK, Feliars D, Sudarshan S, Friedrichs WE, Day RT, New DD, et al. Stabilization of HIF-2 α through redox regulation of mTORC2 activation and initiation of mRNA translation. *Oncogene* 2013;32:3147–55.
36. Nilsson H, Jögi A, Beckman S, Harris AL, Poellinger L, Pahlman S. HIF-2 α expression in human fetal paraganglia and neuroblastoma: relation to sympathetic differentiation, glucose deficiency, and hypoxia. *Exper Cell Res* 2005;303:447–56.
37. Chantry YH, Gustafson WC, Itsara M, Persson A, Hackett CS, Grimmer M, et al. Paracrine signaling through MYCN enhances tumor-vascular interactions in neuroblastoma. *Sci Translat Med* 2012;4:115ra3.
38. Chesler L, Schlieve C, Goldenberg DD, Kenney A, Kim G, McMillan A, et al. Inhibition of phosphatidylinositol 3-kinase destabilizes Mycn protein and blocks malignant progression in neuroblastoma. *Cancer Res* 2006;66:8139–46.
39. Johnsen JL, Segerström L, Orrego A, Elfman L, Henriksson M, Kagedal B, et al. Inhibitors of mammalian target of rapamycin downregulate MYCN protein expression and inhibit neuroblastoma growth in vitro and in vivo. *Oncogene* 2008;27:2910–22.
40. Morrow CJ, Gray A, Dive C. Comparison of phosphatidylinositol-3-kinase signalling within a panel of human colorectal cancer cell lines with mutant or wild-type PIK3CA. *FEBS Lett* 2005;579:5123–8.
41. Vasudevan KM, Barbie DA, Davies MA, Rabinovsky R, McNear CJ, Kim JJ, et al. AKT-independent signaling downstream of oncogenic PIK3CA mutations in human cancer. *Cancer Cell* 2009;16:21–32.
42. Gan X, Wang J, Su B, Wu D. Evidence for direct activation of mTORC2 kinase activity by phosphatidylinositol 3,4,5-trisphosphate. *J Biol Chem* 2011;286:10998–1002.
43. Humphrey SJ, Yang G, Yang P, Fazakerley DJ, Stockli J, Yang JY, et al. Dynamic adipocyte phosphoproteome reveals that Akt directly regulates mTORC2. *Cell Metab* 2013;17:1009–20.
44. Shanmugasundaram K, Block K, Nayak BK, Livi CB, Venkatachalam MA, Sudarshan S. PI3K regulation of the SKP-2/p27 axis through mTORC2. *Oncogene* 2013;32:2027–36.
45. Tato I, Bartrons R, Ventura F, Rosa JL. Amino acids activate mammalian target of rapamycin complex 2 (mTORC2) via PI3K/Akt signaling. *J Biol Chem* 2011;286:6128–42.
46. Wahane SD, Hellbach N, Prentzell MT, Weise SC, Vezzali R, Kreutz C, et al. PI3K-p110 α -subtype signalling mediates survival, proliferation and neurogenesis of cortical progenitor cells via activation of mTORC2. *J Neurochem* 2014;130:255–67.
47. Hidalgo M, Amant F, Biankin AV, Budinska E, Byrne AT, Caldas C, et al. Patient-derived xenograft models: an emerging platform for translational cancer research. *Cancer Discov* 2014;4:998–1013.
48. Lin Q, Cong X, Yun Z. Differential hypoxic regulation of hypoxia-inducible factors 1 α and 2 α . *Mol Cancer Res* 2011;9:757–65.
49. Pietras A, Hansford LM, Johnsson AS, Bridges E, Sjölund J, Gisselsson D, et al. HIF-2 α maintains an undifferentiated state in neural crest-like human neuroblastoma tumor-initiating cells. *Proc Natl Acad Sci U S A* 2009;106:16805–10.
50. Polivka J Jr., Janku F. Molecular targets for cancer therapy in the PI3K/AKT/mTOR pathway. *Pharmacol Ther* 2014;142:164–75.